Reproducibility of axon reflex-related vasodilation assessed by dynamic thermal imaging in healthy subjects

M.D. Nieuwenhoff [a],[*],[1], Y. Wu [b],[1], F.J.P.M. Huygen [a], A.C. Schouten [b],[c], F.C.T. van der Helm [b], S.P. Niehof [a]

[a] Department of Anesthesiology and Pain Medicine, Erasmus MC University Medical Center, Room Ba-430, P.O. box 2040, 3000CA Rotterdam, The Netherlands
[b] Department of Biomechanical Engineering, Delft University of Technology, Mekelweg 2, 2628CD Delft, The Netherlands
[c] Department of Biomechanical Engineering, MIRA Institute, University of Twente, Building Zuidhorst, P.O. box 217, 7500AE Enschede, The Netherlands

A B S T R A C T

Introduction: Small nerve fiber dysfunction is an early feature of diabetic neuropathy. There is a strong clinical need for a non-invasive method to assess small nerve fiber function. Small nerve fibers mediate axon reflex-related vasodilation and play an important role in thermoregulation. Assessing the reflex vasodilation after local heating might elucidate some aspects of small fiber functioning. In this study, we determined the reproducibility of the reflex vasodilation after short local heating in healthy subjects, assessed with thermal imaging and laser Doppler imaging.
Methods: Healthy subjects underwent six heating rounds in one session (protocol I, N = 10) or spread over two visits (protocol II, N = 20). Reflex vasodilation was elicited by heating the skin to 42 °C with an infrared lamp. Skin temperature and skin blood flow were recorded during heating and recovery with a thermal imaging camera and a laser Doppler imager. Skin temperature curves were fitted with a mathematical model to describe the heating and recovery phase with time constant tau (tau_{Heat} and tau_{Cool1}).
Results: The reproducibility of tau within a session was moderate to excellent (intra-class correlation coefficient 0.42–0.86) and good (0.71–0.72) between different sessions. Within one session the differences in tau_{Heat} were small (bias ± SD −1.3 ± 18.9 s); the bias between two visits was −1.2 ± 12.2 s. For tau_{Cool1} the differences were also small, 1.4 ± 6.6 s within a session and between visits −1.4 ± 11.6 s.
Conclusions: The heat induced axon reflex-related vasodilation, assessed with thermal imaging and laser Doppler imaging, was reproducible both within a session and between different sessions. Tau describes the temporal profile in one parameter and represents the effects of all changes including blood flow and as such, is an indicator of the vasodilator function. tau_{Heat} and tau_{Cool1} can accurately describe the dynamics of the axon reflex-related vasodilator response in the heating and recovery phase respectively.

Introduction

Neuropathy is a common complication of diabetes, and is often accompanied by pain (Veves et al., 2008). One of the earliest features of diabetic neuropathy is small nerve fiber damage, which likely precedes large fiber involvement (Tavakoli et al., 2010; Vas and Rayman, 2013). Small nerve fibers are sensitive to temperature, play an important role in thermoregulation and mediate axon reflex-related vasodilation (the initial part of the vasomotor response). Small nerve fiber function is altered in diabetes and diabetic neuropathy (Charkoudian, 2003; Minson et al., 2001; Stephens et al., 2001). Assessment of small nerve fiber function remains a challenge, however there is a strong clinical need for parameters describing the (dys)function of these nerve fibers.

Various tests are available to assess small nerve fibers. Skin biopsy and corneal confocal microscopy can be used to assess small fiber structure; thermal tests and laser Doppler can be used to assess small fiber function (Tavakoli et al., 2010; Vas and Rayman, 2013; Cruccu et al., 2010). Both skin biopsy and corneal confocal microscopy have limitations and only assess small fiber structure, not function. Thermal testing detects temperature- and pain-thresholds, but is inherently subjective as it depends on the subject's perception. The laser Doppler and the laser Doppler flare method are often used together with heat for heat induced reflex vasodilation (Vas and Rayman, 2013; Caselli et al., 2006; Illigens et al., 2013; Namer et al., 2013). The majority of studies use a contact heating element to warm the skin. This obstructs direct measurement of the heated area during the heating phase and information on small fiber function is only gathered after the heating phase has

---

ended. Furthermore, the depth of heating and influence of pressure of the heating block on the local blood flow are unknown.

Static thermal imaging has also been used to study vasomotor responses. Sun et al. (2006) found skin temperature differences to identify sympathetic damage in diabetic feet. Thermal imaging can also measure dynamic responses, i.e. the temperature course in relation to a perturbation such as heating. Dynamic thermal imaging has been used to study vasomotor responses (Nielsen et al., 2013; Gazerani and Arendt-Nielsen, 2011), however the use of a contact-heat element results in the same limitations mentioned above. Other heating methods, such as infrared heating, have not been studied before in combination with thermal imaging. In addition, results are often expressed as absolute values or percentage increase over baseline. This does not allow description of the pattern of the temperature curve and severely limits extraction of information on dynamics of the nerve and blood flow response from the whole curve. Therefore, the temperature curves should be assessed using mathematical models that can reflect more of the ongoing physiology (Merla et al., 2002a). Shortened local heating protocols have been used to specifically focus on the axon reflex part of the vasomotor response (Huang et al., 2012) to allow for repeated measurements in a relatively short period of time.

We developed a set-up in which non-contact heating with an infrared lamp evokes axon reflex-related vasodilation. A mathematical model described the skin temperature curve to quantify the dynamics of the response in a clinically potential relevant parameter. Impaired small nerve fiber function and reflex vasodilation could result in an altered skin temperature curve and a decreased skin blood flow response, i.e. slower recovery. The aim of this study is to determine the reproducibility of the axon reflex-related vasodilation after short local heating in healthy subjects, assessed with thermal imaging and laser Doppler imaging. In the future, this methodology can be used in diabetic and other neuropathy subjects to assess axon reflex-related vasodilation and small fiber function.

Methods

After obtaining approval from the Institutional Ethics Committee (ref NL33823.078.10), 28 healthy adult volunteers were enrolled. All subjects provided written informed consent. The subjects were free of neurological or vascular disorders and other conditions which may affect the vasomotor response. Also subjects had to refrain from smoking, caffeine and alcohol containing beverages for at least six hours prior to the measurements. The experiment consisted of two different protocols, 10 subjects participated in protocol I and 20 subjects participated in protocol II. Two of the subjects participated in both protocols.

Experimental setup and measurements

All measurements were performed in a temperature-controlled room (21–25 °C) with steady illumination. Subjects acclimatized to the room for at least 15 min before the start of measurements. The experimental setup consisted of an infrared lamp (Hydrosun 750 infrared lamp with Schott BG780 optical filter, Hydrosun Medizintechnik GmbH, Müllheim, Germany), a laser Doppler imager (LDI) (Periscan PIM3 system, Perimed, Järfälla, Sweden), a thermal imaging camera (FLIR SC5600, FLIR Systems Inc., Wilsonville, USA) and custom made Matlab scripts (Matlab R2012a, The Mathworks, Natick, USA) for analysis.

The skin was heated with the infrared lamp, with the hand in the center of the lamp's heating field at a distance of 20 cm. Skin blood flux was measured with the LDI at a scanning distance of 40 cm. The scan area was set to 2×2 cm, i.e. a resolution of 1.6 mm (with 12 by 13 pixels) on the skin, which resulted in a scan rate of 11 images/min. The perfusion is measured in arbitrary perfusion units (PU) and the accuracy is the measured value $\pm 10\%$.

The thermal imaging camera measured skin temperature from approximately 60 cm distance from the skin surface, at 5 Hz with a resolution of 640 by 512 pixels (approximately 16.0 cm by 12.8 cm) and a temperature resolution of 0.02 °C, skin emissivity was set to 0.96. Skin blood flux and skin temperature were recorded simultaneously.

Protocols

We applied two different protocols: to investigate agreement between hands in a single session and to investigate agreement between different sessions. The timeline of the protocols is illustrated in Fig. 1. Skin temperature and skin blood flow baseline values were recorded for one minute before the infrared lamp was switched on to heat the dorsum of the hand up to 42 °C (heating phase). When the skin temperature reached 42 °C (a small center area in the thermal picture), the lamp was switched off. The measurement continued for nine minutes, to record the natural skin cooling and the skin blood flow response (recovery phase). Between measurements there was a five minute resting period before the next cycle commenced.

In *protocol I* Right vs. Left, each subject had three repetitive measurements of the right hand ($M0_{Right}$, $M1_{Right}$, $M2_{Right}$) directly followed by three measurements of the left hand ($M0_{Left}$, $M1_{Left}$, $M2_{Left}$). In *protocol II* Interval repeated measurements, each subject had three repetitive measurements of the right hand (Visit 1: $M0_{Right}$, $M1_{Right}$, $M2_{Right}$), the measurements were repeated after 7 ± 1 days to assess variation in response over time (Visit 2: $MR0_{Right}$, $MR1_{Right}$ and $MR2_{Right}$ respectively). For Protocol II data on thermal imaging only was recorded, LDI data were not acquired.

Data analysis

Fig. 2 illustrates the skin temperature and skin blood flow curve and the different parameters which are derived from these measurements, describing the heating phase and recovery phase. Skin temperature was analyzed offline, the analysis procedure is described in detail in Appendix A. In brief, heat time, baseline and peak skin temperatures were obtained from the thermal imaging data. Thereafter the actual temperature curve was fitted with a mathematical model in order to obtain the time constant (tau). Physically, tau describes how fast a system responds to adapt to a new situation. In our experiment Tau reflects changes in the energy exchange. During heating the energy of the lamp has the largest contribution. During the recovery phase energy is dissipated mainly through radiation and skin blood flow. A high tau value indicates a slow change and a low tau a fast change. To fit the model, the temperature curve was divided into different sections: (1) during heating from 39 °C until the lamp was switched off (~42 °C) (phase Heat); (2) the early recovery phase from lamp switch off (~42 °C) until 39 °C (phase Cool 1); and (3) the late recovery phase from 39 °C until 37 °C (phase Cool 2). Cutoff points for these sections were selected based on reports that the onset of vasodilation occurs around 39 °C (Magerl and Treede, 1996), and axon reflex regulation of skin temperature is active above 37 °C (Magerl and Treede, 1996; Barcroft and Edholm, 1943).

Statistical analysis

Statistical analysis was performed using SPSS version 21 for Windows (SPSS Inc., USA), graphs were drawn with GraphPad Prism version 5 (GraphPad Software Inc., USA) or Matlab. Results are presented as mean with standard deviation (mean $\pm$ SD) unless stated otherwise. Variation in response between measurements was analyzed with repeated measures ANOVA with Bonferroni correction for factors of skin blood flow and skin temperature. For protocol I measurements were compared within a hand and compared between hands per measurement (e.g. $M0_{Right}$ vs. $M0_{Left}$). For protocol II measurements were compared within a session and between sessions (e.g. $M0_{Right}$ vs. $MR0_{Right}$). For skin temperature at the 15% amplitude of the LDI signal the 95% confidence interval was calculated ($CI_{95\%}$). Reproducibility was assessed

Fig. 1. Protocol timeline. After a 15 min acclimation period, the measurements start. One measurement consists of three phases: the baseline (B, 1 min), heating phase (up to 42 °C) and a recovery phase (9 min), followed by a 5 min rest. The measurements are executed in cycles of 3 measurements.

using intraclass correlation coefficient (ICC). An ICC of 0.8 to 1 was considered as excellent, 0.6 to 0.79 good, 0.4 to 0.59 as moderate. Agreement between measurements was visualized by means of Bland–Altman plots. A p-value of <0.05 was considered statistically significant. Missing values and outliers were excluded from analysis. The root mean square error (RMSE) was calculated to determine the accuracy of the model fit.

Results

The characteristics of the subjects are summarized in Table 1. In Fig. 2 skin temperature and skin blood flow of a single measurement of one subject are presented. After the start of heating, skin temperature immediately increases, and after approximately 30 s skin blood flow increases too. In the recovery phase, skin temperature and skin blood flow gradually decrease towards a steady state.

Protocol I Right vs. Left

At the beginning of the experiment, the mean room temperature was 22.3 ± 0.4 °C and increased to 23.1 ± 0.3 °C ($p < 0.001$) at the start of $M0_{Left}$. Thermal imaging, laser Doppler and fitting results are presented in Table 2. Heating time within the first hand (right) was approximately 30% longer in the first measurement ($M0_{Right}$), compared to $M1_{Right}$ and $M2_{Right}$. This was not observed within the second (left) hand. In the right hand, baseline skin temperature increased after the first measurement ($p < 0.05$), whereas it was not different within the left hand. At 15%amplitude of the LDI signal the corresponding skin
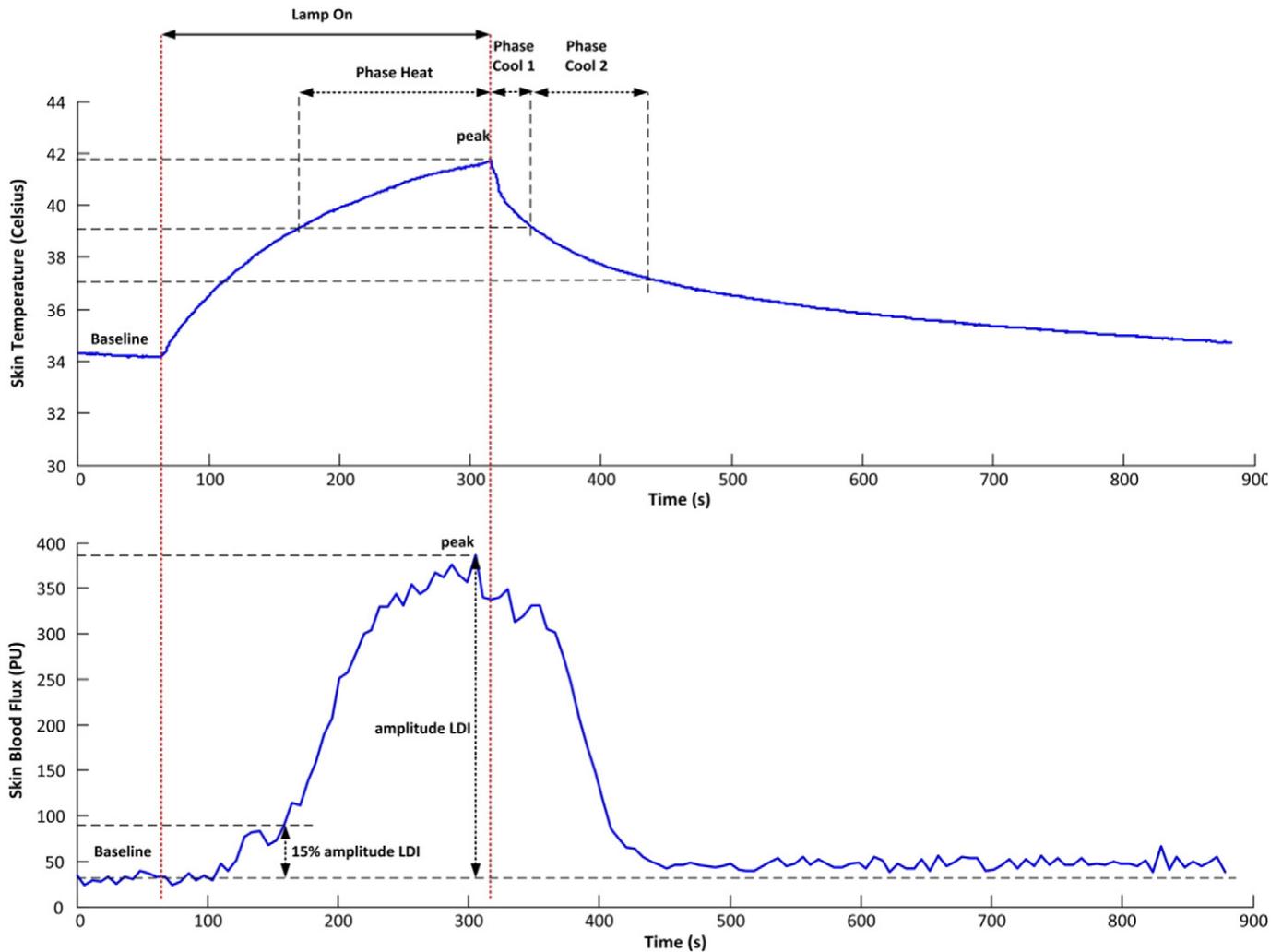

Fig. 2. Skin temperature and blood flux curves of one measurement in one subject. The top figure shows the skin temperature curve, the bottom figure the corresponding skin blood flux. Baseline is measured for one minute, followed by switching on the lamp to heat the skin to ~42 °C, then the lamp is switched off and the recovery is measured. In the skin temperature curve three phases are identified based on temperature. Phase Heat, during the heating phase [39 °C to ~42 °C]: Phase Cool 1, initial recovery phase [~42 °C to 39 °C]: Phase Cool 2, second recovery phase [39 °C to 37 °C]. From the laser Doppler data baseline, peak, amplitude and 15%amplitudeLDI values are extracted. The skin temperature corresponding to the 15%amplitudeLDI point was defined as the onset of vasodilation.

Table 1
Subject characteristics per protocol.

	Protocol I (n = 10)	Protocol II (n = 20)
Male/female	3/7	10/10
Age (years)	27.8 ± 2.2	25.1 ± 3.4
Body mass index (kg/m^2)	22.5 ± 2.7	23.1 ± 2.3
Smoker	0	1
Dominant hand (R/L)	9/1	18/2
Systolic blood pressure (mm Hg)	118 ± 8	124 ± 10
Diastolic blood pressure (mm Hg)	67 ± 6	78 ± 10

temperature for the right hand was 39.2 ± 1.3 °C (CI$_{95\%}$ 38.7–39.6 °C) vs. 39.4 ± 0.9 °C (CI$_{95\%}$ 39.1–39.7 °C) in the left hand.

The time course of the temperature profile was described with tau. Higher tau indicates slower change. Tau$_{Heat}$ was higher than tau$_{Cool1}$ indicating that temperature change in the late heating phase is slower than in the recovery phase. Mean RMSE for tau$_{Heat}$ and tau$_{Cool1}$ were 0.14 °C and 0.26 °C respectively. Tau correlated for heating (phase Heat: Spearman r = 0.43, p = 0.02) and the recovery phase (Cool 1: Spearman r = 0.70, p < 0.001). For tau$_{Heat}$ the overall ICC (all 6 measurements) was 0.42, for tau$_{Cool1}$ the overall ICC was 0.60. The ICC for tau$_{Heat}$ within a hand was 0.60 in the right hand and 0.58 in the left hand. For tau$_{Cool1}$ the ICC was 0.62 and 0.78 in the right and left hand respectively. Agreement between repeated measurements for tau in the heating phase (tau$_{Heat}$) and in the initial cooling phase (tau$_{Cool1}$) is plotted in a Bland–Altman graph (Fig. 3A + B), the bias ± SD was −1.3 ± 18.9 s and 1.4 ± 6.6 s respectively. Tau values at the end of the recovery phase (tau$_{Cool2}$) had a very large spread (data not shown).

Protocol II Interval repeated measurements

Measurements were performed in the right hand on two separate visits. Thermal imaging and fitting results are presented in Table 3. On both visits the heating time of the initial measurement, M0$_{Right}$ and MR0$_{Right}$ respectively, took more time than the subsequent rounds to heat up to 42 °C. There was no significant difference in heating time between the two visits. Mean baseline skin temperature increased with approximately 2 °C after the initial measurement M0$_{Right}$, this was also the case within the second visit. Tau$_{Cool1}$ increased after the initial measurement. Mean RMSE for tau$_{Heat}$ and tau$_{Cool1}$ were 0.20 °C and 0.30 °C respectively. For tau$_{Heat}$ the overall ICC (all 6 measurements) was 0.71, for tau$_{Cool1}$ the overall ICC was 0.72. The within session ICC for tau$_{Heat}$ was 0.70 for visit 1 and 0.79 for visit 2. For tau$_{Cool1}$ the within session ICC was 0.86 for visit 1 and 0.84 for visit 2. Agreement between visits for tau$_{Heat}$ and tau$_{Cool1}$ is plotted in a Bland–Altman graph (Fig. 3C + D), the bias ± SD was −1.2 ± 12.2 s and −1.4 ± 11.6 s respectively. Tau values at the end of the recovery phase (tau$_{Cool2}$) had a very large spread (data not shown).

Discussion

The reproducibility of axon reflex-related vasodilation assessed with thermal imaging and laser Doppler imaging is good. The dynamics of the vasomotor response can be accurately described with tau$_{Heat}$ and tau$_{Cool1}$ during the heating and recovery phase respectively. Tau is reproducible cycle after cycle, and between two sessions a week apart.

We quantified the thermal response by fitting a model to describe the heating and recovery curve with one factor (tau). We found that tau was reproducible both within a session and between different occasions of measurements, for temperatures above 39 °C. Reproducibility of skin vasodilation has been assessed by others (Huang et al., 2012; Tew et al., 2011; Roustit et al., 2010) using different setups and parameters, making it difficult to compare these results to our study. Tew et al. (2011) found an ICC of 0.54 and a bias of −3 (limits of agreement −25 to 20) for inter-day reproducibility of the initial peak of laser Doppler, expressed as percentage of the maximal cutaneous vascular conductance. The between visit ICC we found is higher, the bias and limits of agreement are similar to the difference found in our study. However they did not investigate the reproducibility between multiple measurements per session. Within session ICC was higher in protocol II compared to protocol I, we do not have an explanation for the observed difference in ICC.

For skin temperature below 39 °C, tau variation increased enormously, probably because of the passive nature (skin blood flow did not alter) in this phase and the variation between subjects in passive thermodynamic parameters, and no useful information could be identified because of this variation.

Furthermore we found that tau$_{Cool1}$ differs between measurements. Tau$_{Cool1}$ in the initial measurement (M0) is lower than in the subsequent rounds. This phenomenon is also present one week later and a similar pattern is seen in the Right vs. Left protocol. The underlying mechanism is unknown. Because the difference is also present in the second hand within a single session, this suggests that it is likely caused by a local process. It is also unlikely that this difference is caused by changes in baseline skin temperature or skin blood flow, because no changes in these parameters were observed in the left hand (Right vs. Left protocol) while tau$_{Cool1}$ increased. We speculate that energy storage in deeper tissue layers is the cause of the observed difference. Others (Wilson and Spence, 1988; Frahm et al., 2010) have used temperature distribution models to estimate temperature in deeper tissue layers and concluded that temperature change may be ongoing even after removal of the stimulus. Another explanation for part of the observed difference could be that we applied repeated heating with short intervals in our study. Some (Frantz et al., 2012; Ciplak et al., 2009) but not others (Del Pozzi and Hodges, 2015) report a different response following repeated local heating. This effect should be investigated in future research.

Application of infrared heat resulted in a significant increase in skin temperature and skin blood flow, this is in agreement with previous

Table 2
Protocol I Right vs. Left — thermal imaging, laser Doppler imaging and fitting results.

	M0$_{Right}$	M1$_{Right}$	M2$_{Right}$	M0$_{Left}$	M1$_{Left}$	M2$_{Left}$
Heating time (s)	311 ± 86	227 ± 84[*]	228 ± 77[*]	231 ± 86[*]	211 ± 67	239 ± 85
Skin temperature baseline (°C)	34.0 ± 1.2	35.0 ± 0.8[*]	34.8 ± 0.7[*]	34.1 ± 1.0	34.3 ± 0.8	34.2 ± 0.9
Skin temperature peak (°C)	41.8 ± 0.8	41.9 ± 0.4	42.1 ± 0.4	41.7 ± 0.3	41.8 ± 0.6	41.9 ± 0.6
LDI baseline (PU)	56 ± 15	68 ± 14	58 ± 11	43 ± 17	46 ± 20	43 ± 17
LDI peak (PU)	366 ± 98	320 ± 57	344 ± 72	386 ± 150	350 ± 166	354 ± 133
Increase LDI over baseline (%)	677 ± 170	499 ± 175	618 ± 171	1040 ± 547[*]	852 ± 430	936 ± 446
Tau$_{Heat}$ (s)	94.7 ± 23.3	97.6 ± 19.7	93.8 ± 15.0	93.0 ± 8.0	96.5 ± 11.7	100.5 ± 11.5
Tau$_{Cool1}$ (s)	35.9 ± 10.2	37.8 ± 7.7	39.8 ± 7.4	33.9 ± 7.9	37.1 ± 8.1	37.4 ± 7.6

LDI, laser Doppler imager; PU, perfusion units. For tau$_{Cool1}$; in M0$_{Right}$ 1 outlier was excluded.

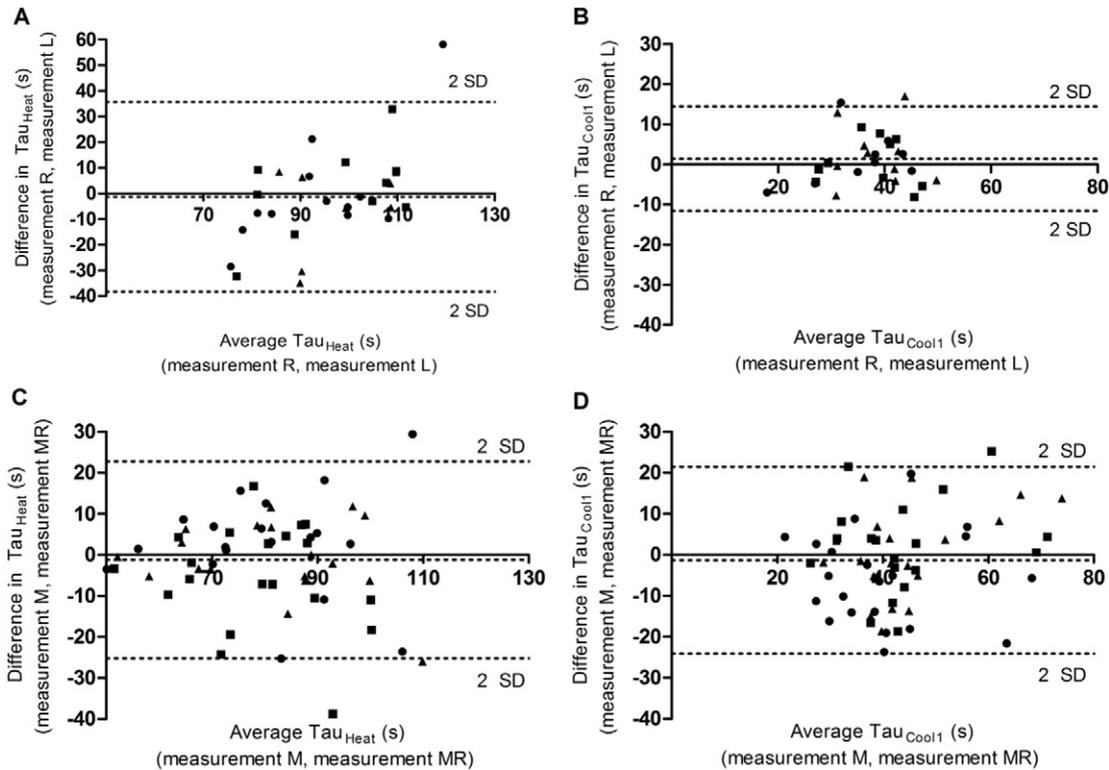[*] p < 0.05 compared to M0$_{Right}$.

Fig. 3. Bland–Altman analysis of tau_{Heat} and tau_{Cool1}. A + B) Protocol I Right vs. Left. Comparison of repeated tau_{Heat} and tau_{Cool1} measurements in the Right vs. the Left hand. C + D) Protocol II Interval repeated measurements. Comparison of tau_{Heat} and tau_{Cool1} measurements on two separate occasions (M vs. MR measurement). Dotted lines represent the bias $\pm$ 2 SD; the bias is the average of the differences. The average of the paired values is plotted on the x-axis and the corresponding difference is plotted on the y-axis. Circles (●) represent the M0 measurement (e.g. $M0_{Right}$ vs. $M0_{Left}$), squares (■) represent the M1 measurement, and triangles (▲) represent the M2 measurement.

reports by others using various heating paradigms (Gazerani and Arendt-Nielsen, 2011; Huang et al., 2012; Johnson and Kellogg, 2010). The initial skin blood flow peak mediated via the sensory afferents occurs after approximately 3–5 min of heating. The nitric oxide (NO) mediated phase starts approximately 10 min after the onset of heating (Charkoudian, 2003). In our study the mean heating time ranged from 3.5–7 min, as this is well under 10 min it is unlikely that NO mediated vasodilation was initiated. Also in none of the subjects a nadir or second peak was observed. Therefore, we believe the sensory afferents are the major contributors to the response we observed in this experiment and the contribution of NO, if present at all, is small.

Differences in skin temperature curve waveforms in the heating and recovery phase are precisely described by tau. The differences observed in heating and recovery are largely caused by changes in skin blood flow. Skin blood flow is at its peak around 42 °C, transferring heat away from the skin surface. This resulted in a higher tau for the heating phase compared to the recovery phase, i.e. quicker change in the recovery phase compared to the heating phase. The onset of vasodilation (skin temperature at the 15%amplitudeLDI point), set-in around

39.3 °C. Magerl and Treede (1996)) found that slowly rising heat induced vasodilation at 39.6 °C, this is slightly higher than the 39.3 °C we found but the difference is probably due to differences in heating protocol, definition of onset of vasodilation and measurement devices.

In the current study we selected a target end temperature and therefore heating time and heating rate were variable. From literature we know that heating rate influences the subsequent skin blood flow response (Hodges et al., 2009). Rapid increases trigger cutaneous pain receptors and alter the response to local heating (Carter and Hodges, 2011). In the current study, the heating rate was slow – modest and below $0.05 \, °C \cdot s^{-1}$ for nearly all measurements. In 10 out of 180 measurements (four subjects) the heating rate was higher (max. $0.078 \, °C \cdot s^{-1}$). None of our subjects reported pain during heating. Also the heating was not rapid, therefore we do not expect that the above described phenomenon played a role in our study. Also the amount of external energy input by the infrared lamp varied, but this did not affect tau [Wu, unpublished observations].

There could also be additional confounding factors which we did not take into account or corrected for. Known factors that influence

Table 3
Protocol II Interval repeated measurements — thermal imaging and fitting results.

	$M0_{Right}$	$M1_{Right}$	$M2_{Right}$	$MR0_{Right}$	$MR1_{Right}$	$MR2_{Right}$
Heating time (s)	422 ± 129	$267 \pm 84^*$	$252 \pm 76^*$	393 ± 122	$242 \pm 81^†$	$238 \pm 61^†$
Skin temperature baseline (°C)	33.1 ± 2.2	$35.3 \pm 1.4^*$	$35.2 \pm 1.1^*$	32.9 ± 2.3	$35.1 \pm 1.1^†$	$35.0 \pm 0.9^†$
Skin temperature peak (°C)	41.7 ± 0.5	42.0 ± 0.3	42.0 ± 0.3	41.7 ± 0.6	41.8 ± 0.5	41.9 ± 0.3
Tau_{Heat} (s)	81.3 ± 16.5	76.2 ± 13.4	80.9 ± 15.4	79.0 ± 16.4	81.5 ± 15.6	82.4 ± 16.9
Tau_{Cool1} (s)	37.3 ± 13.5	$44.7 \pm 13.9^*$	$44.2 \pm 14.8^*$	38.0 ± 11.9	43.1 ± 12.0	$43.5 \pm 10.9^†$

For tau_{Heat}; in $M2_{Right}$ 2 outliers were excluded, in $MR0_{Right}$ 1 outlier was excluded.

[*] $p < 0.05$ compared to $M0_{Right}$.
[†] $p < 0.05$ compared to $MR0_{Right}$.

thermoregulation or cause temperature fluctuations include fast from food intake, exercise and menstrual cycle (Johnson and Kellogg, 2010; Charkoudian et al., 1999). Controlling for some of these factors could reduce variability and enhance the power of this technique.

The next step would be to quantify the axon reflex-related vasodilator response in (diabetic) patients with small fiber dysfunction or vasomotor dysfunction, using this fitting model. We believe patients with small fiber dysfunction will have an altered axon reflex-related response and subsequently a different tau compared to healthy subjects. Fitting routines have been successfully used by others to identify altered vasomotor responses in patients with diabetes (Bandini et al., 2013) and Raynaud's (Merla et al., 2002a, 2002b; Ismail et al., 2014; Mariotti et al., 2009). Showing this methodology could be helpful to quantify the vasomotor response and identify subjects with altered responses. As only hands of young subjects were studied, caution should be taken to extrapolate these results to other body regions and older subjects.

Conclusion

The heat induced axon reflex-related vasodilation, assessed with thermal imaging and laser Doppler imaging, is reproducible both within a session and between different sessions. Tau describes the temporal profile in one parameter and represents the effects of all changes including blood flow and as such, is an indicator of the vasodilator function. Tau$_{Heat}$ and tau$_{Cool1}$ can accurately describe the dynamics of the axon reflex-related vasodilator response in the heating and recovery phase respectively. This methodology can be applied in neuropathy patients in an effort to monitor and quantify small nerve fiber function and axon reflex-related vasodilation.

Conflicts of interests

The authors declare they have no conflicts of interests.

Author's contribution

MN and YW were involved in the design of the experiments, collection, analysis and interpretation of data, and drafted the manuscript. FJH participated in the concept and design of the experiments and critically revised the manuscript. AS participated in the analysis and interpretation of data and drafting of the manuscript. FCH participated in the design and critically revised the manuscript. SN conceived of the study, and participated in its design and helped to draft the manuscript. All authors read and approved the final manuscript.

Acknowledgments

Appendix A

Temperature of the skin is related to energy stored in the skin. The higher the energy that is stored in the skin the higher the skin temperature. The energy that is stored in the skin (S) is related to energy that is imposed on the skin (Q$_i$) plus the metabolic heat production (M). Depending on the temperature, energy is also lost or gained through skin-environment radiation (Q$_{s-e}$) and internal heat conduction of the skin (C). A final term in the energy balance is energy gained or lost through blood flow (F). This can be expressed in a general balance energy equation of the skin surface

$$S = Q_i + M + Q_{s-e} + C + F. \tag{1}$$

The change in the energy stored in the skin (S) induces the change in the skin temperature:

$$S = \rho c \frac{dT_{sf}}{dt} \tag{2}$$

where T_{sf} is the skin temperature in units of Kelvin, t time and c the thermal capacity of the skin.

In the right side of Eq. (1), Q$_i$ is constant and mainly determined by the lamp radiation during the heating phase, and is equal to zero in the cooling phase. The metabolic heat (M) is assumed constant all the time.

$$Q_{s-e} = \varepsilon\sigma\left(T_{sf}^4 - T_e^4\right) \tag{3}$$

where ε is the emissivity of the skin, σ is Stefan–Boltzmann constant, T_e is the room temperature in the unit of Kelvin. In our case, Q$_{s-e}$ can be further approximated as a linear function:

$$Q_{s-e} \approx \alpha T_{sf} + \beta. \tag{4}$$

In which α and β are two constants.

C is derived from the work of Fujimasa and Pavlidis (Fujimasa et al., 2000; Pavlidis and Levine, 2002).

$$C = (K/3D) \times \frac{dT_{sf}}{dt} \tag{5}$$

where K is the thermal conductivity of the skin, D is the depth of the core temperature point from the skin surface.

$$F = \omega_b c_b\left(T_b - T_{sf}\right) \tag{6}$$

In which ω_b is the skin blood flow, c_b the thermal capacity of the blood, T_b is the temperature of the skin blood in the unit of Kelvin. The skin blood flow removes the energy in the skin when the skin temperature is higher than the blood temperature, and brings energy when the skin temperature is lower than the blood temperature.

Eq. (1) can be converted into an approximated linear function dependent on the skin temperature:

$$\frac{dT_{sf}}{dt} \approx AT_{sf} + B. \tag{7}$$

In which

$A = (\alpha - \omega_b c_b)/(\rho c - K/3D)$ and
$B = (Q_i + M + \beta + \omega_b c_b T_b)/(\rho c - K/3D)$.

The solution to Eq. (7) is

$$T_{sf} = -\frac{B}{A} + \left(T_0 + \frac{B}{A}\right)e^{At} \tag{8}$$

or

$$T_{sf} = \tau B + (T_0 - \tau B)e^{-t/\tau}. \tag{9}$$

In which $T_0 = T_{sf}(t = 0)$ and $\tau = -1/A$. The time constant tau (τ) indicates the rate of the dynamic change in the skin temperature during the heating and the cooling. Values were obtained through a least square curve fitting method. Eq. (9) is considered as the general function form of the skin temperature, a computer program in MATLAB was made to input a set of possible values for τ and B, and to compare the

modeled skin temperature with the measured skin temperature. The quality of the curve fitting was indicated by the root mean square error (RMSE). The values of τ and B were obtained when the best curve fitting (minimum RMSE) was found.

References

Bandini, A., et al., 2013. Effect of local blood flow in thermal regulation in diabetic patient. Microvasc. Res. 88, 42–47 (July).

Barcroft, H., Edholm, O.G., 1943. The effect of temperature on blood flow and deep temperature in the human forearm. J. Physiol. 102 (1), 5–20.

Carter, S.J., Hodges, G.J., 2011. Sensory and sympathetic nerve contributions to the cutaneous vasodilator response from a noxious heat stimulus. Exp. Physiol. 96 (11), 1208–1217.

Caselli, A., et al., 2006. Validation of the nerve axon reflex for the assessment of small nerve fibre dysfunction. J. Neurol. Neurosurg. Psychiatry 77 (8), 927–932.

Charkoudian, N., 2003. Skin blood flow in adult human thermoregulation: how it works, when it does not, and why. Mayo Clin. Proc. 78 (5), 603–612.

Charkoudian, N., et al., 1999. Influence of female reproductive hormones on local thermal control of skin blood flow. J. Appl. Physiol. 87 (5), 1719–1723.

Ciplak, M., et al., 2009. The vasodilatory response of skin microcirculation to local heating is subject to desensitization. Microcirculation 16 (3), 265–275.

Cruccu, G., et al., 2010. EFNS guidelines on neuropathic pain assessment: revised 2009. Eur. J. Neurol. 17 (8), 1010–1018.

Del Pozzi, A.T., Hodges, G.J., 2015. To reheat, or to not reheat: that is the question: the efficacy of a local reheating protocol on mechanisms of cutaneous vasodilatation. Microvasc. Res. 97 (Jan), 47–54.

Frahm, K.S., et al., 2010. Spatial temperature distribution in human hairy and glabrous skin after infrared CO_2 laser radiation. Biomed. Eng. Online 9, 69.

Frantz, J., et al., 2012. Desensitization of thermal hyperemia in the skin is reproducible. Microcirculation 19 (1), 78–85.

Fujimasa, I., Chinzei, T., Saito, I., 2000. Converting far infrared image information to other physiological data. IEEE Eng. Med. Biol. Mag. 19 (3), 71–76.

Gazerani, P., Arendt-Nielsen, L., 2011. Cutaneous vasomotor reactions in response to controlled heat applied on various body regions of healthy humans: evaluation of time course and application parameters. Int. J. Physiol. Pathophysiol. Pharmacol. 3 (3), 202–209.

Hodges, G.J., et al., 2009. The involvement of heating rate and vasoconstrictor nerves in the cutaneous vasodilator response to skin warming. Am. J. Physiol. Heart Circ. Physiol. 296 (1), H51–H56.

Huang, C.S., Wang, S.F., Tsai, Y.F., 2012. Axon reflex-related hyperemia induced by short local heating is reproducible. Microvasc. Res. 84 (3), 351–355.

Illigens, B.M., et al., 2013. Laser Doppler imaging in the detection of peripheral neuropathy. Auton. Neurosci. 177 (2), 286–290.

Ismail, E., et al., 2014. Differential diagnosis of Raynaud's phenomenon based on modeling of finger thermoregulation. Physiol. Meas. 35 (4), 703–716.

Johnson, J.M., Kellogg Jr., D.L., 2010. Local thermal control of the human cutaneous circulation. J. Appl. Physiol. 109 (4), 1229–1238.

Magerl, W., Treede, R.D., 1996. Heat-evoked vasodilatation in human hairy skin: axon reflexes due to low-level activity of nociceptive afferents. J. Physiol. 497 (Pt 3), 837–848.

Mariotti, A., et al., 2009. Finger thermoregulatory model assessing functional impairment in Raynaud's phenomenon. Ann. Biomed. Eng. 37 (12), 2631–2639.

Merla, A., et al., 2002a. Quantifying the relevance and stage of disease with the tau image technique. IEEE Eng. Med. Biol. Mag. 21 (6), 86–91.

Merla, A., et al., 2002b. Infrared functional imaging applied to Raynaud's phenomenon. IEEE Eng. Med. Biol. Mag. 21 (6), 73–79.

Minson, C.T., Berry, L.T., Joyner, M.J., 2001. Nitric oxide and neurally mediated regulation of skin blood flow during local heating. J. Appl. Physiol. 91 (4), 1619–1626.

Namer, B., et al., 2013. Axon reflex flare and quantitative sudomotor axon reflex contribute in the diagnosis of small fiber neuropathy. Muscle Nerve 47 (3), 357–363.

Nielsen, T.A., et al., 2013. The effect of topical capsaicin-induced sensitization on heat-evoked cutaneous vasomotor responses. Int. J. Physiol. Pathophysiol. Pharmacol. 5 (3), 148–160.

Pavlidis, I., Levine, J., 2002. Thermal image analysis for polygraph testing. IEEE Eng. Med. Biol. Mag. 21 (6), 56–64.

Roustit, M., et al., 2010. Reproducibility and methodological issues of skin post-occlusive and thermal hyperemia assessed by single-point laser Doppler flowmetry. Microvasc. Res. 79 (2), 102–108.

Stephens, D.P., et al., 2001. The influence of topical capsaicin on the local thermal control of skin blood flow in humans. Am. J. Physiol. Regul. Integr. Comp. Physiol. 281 (3), R894–R901.

Sun, P.C., et al., 2006. Relationship of skin temperature to sympathetic dysfunction in diabetic at-risk feet. Diabetes Res. Clin. Pract. 73 (1), 41–46.

Tavakoli, M., et al., 2010. Corneal confocal microscopy: a novel means to detect nerve fibre damage in idiopathic small fibre neuropathy. Exp. Neurol. 223 (1), 245–250.

Tew, G.A., et al., 2011. Reproducibility of cutaneous thermal hyperaemia assessed by laser Doppler flowmetry in young and older adults. Microvasc. Res. 81 (2), 177–182.

Vas, P.R., Rayman, G., 2013. The rate of decline in small fibre function assessed using axon reflex-mediated neurogenic vasodilatation and the importance of age related centile values to improve the detection of clinical neuropathy. PLoS One 8 (7), e69920.

Veves, A., Backonja, M., Malik, R.A., 2008. Painful diabetic neuropathy: epidemiology, natural history, early diagnosis, and treatment options. Pain Med. 9 (6), 660–674.

Wilson, S.B., Spence, V.A., 1988. A tissue heat transfer model for relating dynamic skin temperature changes to physiological parameters. Phys. Med. Biol. 33 (8), 895–912.